Concentration-Dependent Fluorescence Properties of Rhodamine 6G in Titanium Dioxide and Silicon Dioxide Nanolayers

ARTICLE *in* THE JOURNAL OF PHYSICAL CHEMISTRY C · MAY 2012

Impact Factor: 4.77 · DOI: 10.1021/jp3022562

7 AUTHORS, INCLUDING:

Aneta Lewkowicz
University of Gdansk
7 PUBLICATIONS **33** CITATIONS
SEE PROFILE

Beata Grobelna
University of Gdansk
35 PUBLICATIONS **272** CITATIONS
SEE PROFILE

Irina Akopova
University of North Texas HSC at Fort Worth
41 PUBLICATIONS **443** CITATIONS
SEE PROFILE

Ignacy Gryczynski
University of North Texas HSC at Fort Worth
368 PUBLICATIONS **9,441** CITATIONS
SEE PROFILE

THE JOURNAL OF PHYSICAL CHEMISTRY C

Article

pubs.acs.org/JPCC

Concentration-Dependent Fluorescence Properties of Rhodamine 6G in Titanium Dioxide and Silicon Dioxide Nanolayers

Aneta Lewkowicz,[†] Piotr Bojarski,*[,†] Anna Synak,[†] Beata Grobelna,[‡] Irina Akopova,[§] Ignacy Gryczyński,[§] and Leszek Kułak[∥]

[†]Institute of Experimental Physics, University of Gdansk, Wita Stwosza 57, 80-952 Gdańsk, Poland

[‡]Faculty of Chemistry, University of Gdansk, Sobieskiego 18/19, 80-952 Gdańsk, Poland

[§]Health Science Center, Center for Commercialization of Fluorescence Technology, University of North Texas, 3500 Camp Bowie Boulevard, Fort Worth, Texas 76107, United States

[∥]Department of Technical Physics and Applied Mathematics, Gdansk University of Technology, Narutowicza 11/12, 80-952 Gdańsk, Poland

ABSTRACT: Thin films of rhodamine 6G in titanium dioxide ($Rh6G/TiO_2$) and silicon dioxide ($Rh6G/SiO_2$) were synthesized using the sol−gel method. We explored two kinds of matrices as hosts for rhodamine 6G (Rh6G) at different concentrations of the dye. The pronounced effect of the dye concentration on the absorption and fluorescence spectra as well as on time-resolved fluorescence spectra was found. In particular, it was found that the aggregation of the guest dye is significantly weaker in the $Rh6G/TiO_2$ nanolayer. The absence of an isosbestic point in absorption spectra in a silica matrix suggests the formation of higher order aggregates, whereas the changes of absorption profile in $Rh6G/TiO_2$ matrix indicate the formation of dimers. Rh6G aggregates are strongly fluorescent in $Rh6G/TiO_2$ nanolayer, which can be seen from time-resolved and steady-state emission spectra. For $Rh6G/SiO_2$ nanolayers these changes are much less pronounced and concern mostly the red shift of the fluorescence maximum.

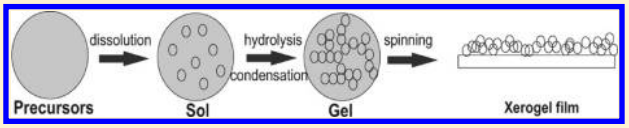

INTRODUCTION

The sol−gel process is an effective technique used for the formation of functional materials starting from a colloidal solution. The sol−gel derived materials can be exploited for different applications, including luminescent materials, potential active media for compact tunable lasers, or functional bioinspired nanomaterials.[1−4] Titanium dioxide is a very important material, for example, in designing new solar cells competitive to the conventional silicon solar cells.[5] Dye-sensitized solar cells (DSSCs) are efficient and cheaper in production than silicon solar cells. A lot of attention involving this subject has been focused on solid-state dye lasers.[6,7] Titanium dioxide is well-known in nanotechnology as a material that provides new opportunities because of its interesting properties, for example, as a semiconductor with rather large forbidden band gap energy of 3.2 eV. This material occurs in three forms: anatase, rutile, and brookite, which enables its applications in electronics, sensor technology, optics, or photocatalysis.[8] In this paper, we use the sol−gel process to obtain and study concentration-dependent fluorescence properties of rhodamine 6G entrapped in titanium dioxide ($Rh6G/TiO_2$) and silicon dioxide ($Rh6G/SiO_2$) nanolayers. Rh6G is a strongly fluorescent dye, the photophysical properties of which have been thoroughly studied at different concentrations in solutions, polymer matrices, glasses, and nanocomposites over past years using mostly steady-state spectroscopic methods.[7−23] In particular, some recent studies of concentration-dependent behavior of Rh6G revealed that its dimers formed in viscous solutions or rigid media can be fluorescent.[16−23] In many recent studies devoted to sol−gel derived luminescent materials, optically and physically thick samples have been prepared and measured. Such results, although very interesting, can be distorted by the presence of inner filter effects (reabsorption and reemission). Therefore, it seems important to find out whether the observed effects originate from the fluorescence of J aggregates. Quite straightforward way to achieve this goal is to prepare sol−gel derived nanolayers doped with a fluorescent dye able to form efficiently aggregates. Such a system, despite the high dye concentration, preserves low optical density, which is the most important condition to neglect inner filter effects.[24] To verify the hypothesis of the fluorescent aggregate formation and to describe well the concentration-dependent properties of $Rh6G/TiO_2$ and $Rh6G/SiO_2$ nanolayers it is necessary to perform both steady-state spectroscopic measurements and time-resolved emission spectra studies. To fill this gap we will study the luminescence properties of well-defined Rh6G-based luminescent hybrid materials in a form of nanolayers using the mentioned methods.

EXPERIMENTAL WORK

Material Synthesis. All reagents used in this study were of analytical grade. [9-(2-Ethoxycarbonylphenyl)-6-(ethylamino)-

Received: March 8, 2012
Revised: May 8, 2012
Published: May 14, 2012

   dx.doi.org/10.1021/jp3022562 | J. Phys. Chem. C 2012, 116, 12304−12311

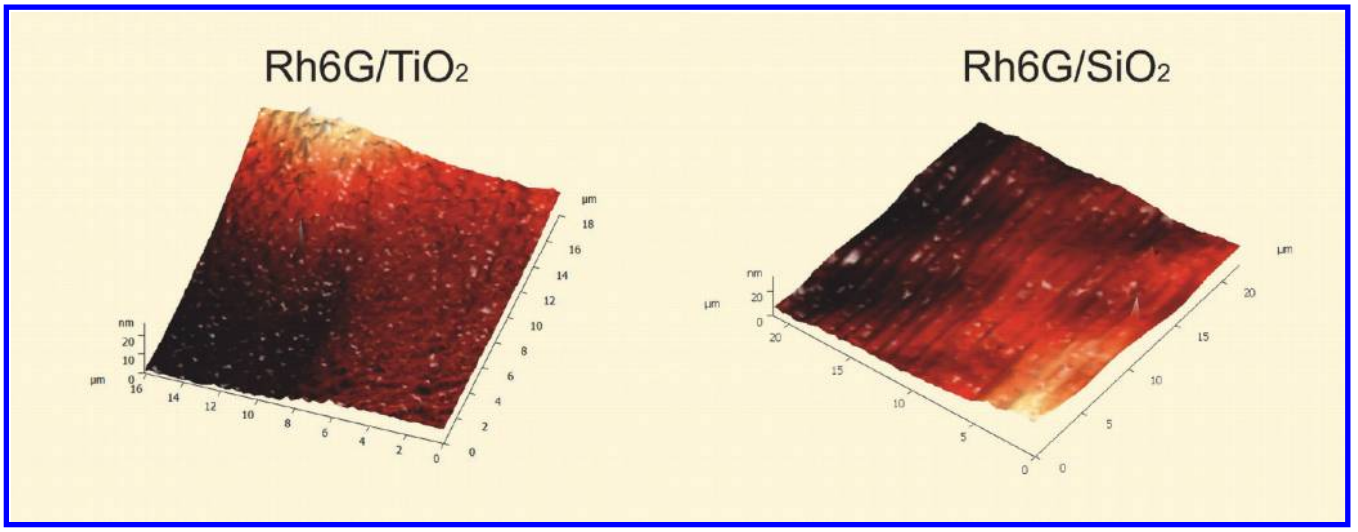

Figure 1. Three-dimensional AFM images for rhodamine 6G at $c = 2 \times 10^{-3}$ mol/dm^3 in two different types of matrices TiO_2 and SiO_2.

2,7-dimethylxanthen-3-ylidene]-ethylazanium chloride (rhodamine 6G) was spectroscopically pure (dye content 99%), and it was purchased from Aldrich (Munich, Germany); tetramethyl orthosilicate (TMOS), titanium(IV) tetra(2-propanolate), poly(ethylene glycol) *p*-(1,1,3,3-tetramethylbutyl)-phenyl ether (Triton X-100), and pentane-2,4-dione were purchased from Aldrich, and propan-2-ol, ethanol, methanol, sodium hydroxide, and hydrochloric acid were purchased from POCH Company (Gliwice, Poland). Deionized water was obtained from a Hydrolab system installed in our laboratory. Rh6G/TiO_2 and Rh6G/SiO_2 thin films (nanofilms) were prepared by the sol−gel method. The precursor solution for Rh6G/TiO_2 was obtained using titanium(IV) tetra(2-propanolate), propan-2-ol, Triton X-100, and hydrochloric acid (37%). Separately, Rh6G was dissolved in ethanol. Next, both solutions were mixed by vigorous stirring. However, the precursor solution for Rh6G/SiO_2 was prepared using tetramethyl orthosilicate and methanol. After a while, Rh6G dissolved in distilled water was added to the solution. Then, three drops of sodium hydroxide (10^{-1} mol/dm^3) as a catalyst were added to promote the reaction of the sol−gel process. Thin films were distributed over a clean piece of a microscopic glass using spin-coating technique (SCI-40 LOT, Oriel spin-coater) at 120 rpm for 60 s. A detailed procedure on thin films preparation can be found in our earlier work.[25] The sol−gel process allows incorporation of Rh6G into titanium dioxide or silicon dioxide matrices at room temperature and atmospheric pressure. Using this method the following concentrations of the dye: 5×10^{-2}, 2×10^{-2}, 10^{-2}, 5×10^{-3}, and 2×10^{-3} mol/dm^3 were obtained. The optical density of the films was in any case below 0.1, which is low enough to neglect the inner filter effects.[24] Thin films were obtained for a couple of different gelation times through the sol−gel method. The gelation time was measured from the moment of mixing all of the components, and it was selected for the purpose of this work as 1, 20, 30, 60, and 90 min.

Apparatus. The absorption spectra were measured with Shimadzu 1650 PC spectrophotometer. Fluorescence spectra were measured upon front face excitation (magic angle mode) with a spectrofluorometer constructed in our laboratory and described earlier.[26] Emission anisotropy was measured with a two-channel single-photon counting polarization spectrofluorometer constructed originally in our laboratory and described previously.[27,28] Time-resolved emission spectra (TRES) were recorded at room temperature with the pulsed spectrofluorometer described previously in detail.[29] The laser system (PL 2143A/SS Nd:YAG laser and the PG 401/SH optical parametric generator emitting pulses of full-width at half-maximum (fwhm) ≈30 ps, E XSPLA, Vilnius, Lithuania), was used as an exciting light source. The 2501S Spectrograph, Bruker Optics Inc. (Billerica, MA) and C4334-01 Streak Camera, Hamamatsu (Hamamatsu City, Japan), constitute a central part of the detection system. All operations are fully automated and controlled by the original Hamamatsu HPDTA software which allows for the real-time data analysis. Atomic force microscopy (AFM) images were collected by scanning dry sample wafers with an atomic force microscope (TMX 2100 Explorer SPM, Veeco, Plainview, NY), equipped with an AFM dry scanner. The AFM scanner was calibrated using a standard calibration grid as well as 100 nm diameter gold nanoparticles. Images were analyzed using SPMLAB software.

RESULTS AND DISCUSSION

The surface topography of the films was studied using the AFM technique. Figure 1 shows the three-dimensional AFM image of Rh6G/TiO_2 and Rh6G/SiO_2 thin film, respectively. The dimensions of the images taken are given in each subfigure. The presented microscopic images are representative for the obtained samples. The thin film appears to be smooth, and its roughness is smaller than 10 nm. The results reveal that the planarity of the prepared thin film is good. The thickness of the thin film was measured as an average value, and it turned out to be about 60 nm in the case of Rh6G/TiO_2 and 75 nm in the case of Rh6G/SiO_2. Rhodamine 6G particles are quite evenly distributed in the matrix.

Figures 2 and 3 show the absorption spectra of Rh6G/TiO_2 (Figure 2) and Rh6G/SiO_2 (Figure 3) nanolayers at several selected concentrations of the dye at room temperature, T = 293 K. It can be seen from both figures that the absorption spectrum evolves with concentration in a way typical of aggregate formation. The observed changes in absorption spectra are much stronger for Rh6G/SiO_2 (Figure 3) than for Rh6G/TiO_2 (Figure 2) matrix at the same dye concentration. The formation of a new absorption band with a maximum at around 500 nm can be seen with the increase in concentration

dx.doi.org/10.1021/jp3022562 | J. Phys. Chem. C 2012, 116, 12304−12311

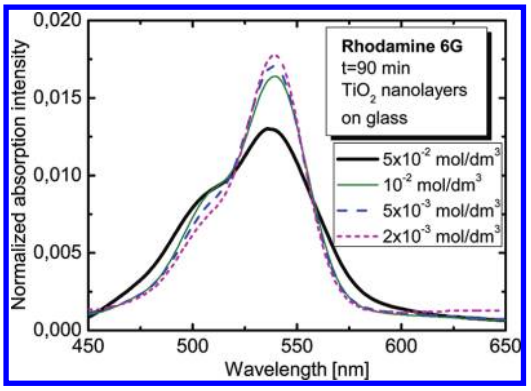

Figure 2. Absorption spectra of Rh6G/TiO_2 nanolayers at several selected concentrations of the dye at room temperature T = 293 K.

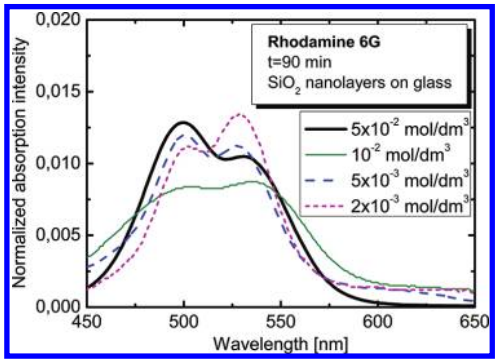

Figure 3. Absorption spectra of Rh6G/SiO_2 (see also Figure 2) nanolayers at several selected concentrations of the dye at room temperature T = 293 K.

in both cases. Simultaneously, the intensity decrease of the monomer absorption band with its maximum around 530 nm can be seen with increasing dye concentration. These regularities are accompanied by the increased halfwidth of absorption spectra at highest concentrations (Table 1).

Table 1. Halfwidths of Absorption Spectra for Rh6G/SiO_2 and Rh6G/TiO_2 at Several Dye Concentrations

c (mol/dm^3)	$\Delta\lambda_{1/2}$ (nm) Rh6G/SiO_2	$\Delta\lambda_{1/2}$ (nm) Rh6G/TiO_2
0.05	92	74
0.005	89	52
0.002	61	44

In the case of Rh6G/SiO_2 matrices we have not found any well-defined isosbestic points between both maxima of the bands (500 and 530 nm) when analyzing the absorption spectra family of Rh6G, suggesting the formation of higher order aggregates rather than simple dimers. Qualitatively similar results can be found for Rh6G in aqueous solutions, where at sufficiently high concentrations the clear formation of higher order aggregates has been found.[9] With this respect we observed somewhat different regularities for Rh6G/TiO_2 nanofilms, where a well-defined isosbestic point can be seen at around 520 nm and the second one at about 558 nm suggesting the formation of H and J dimers. These latter results correspond well to the previous observations performed in poly(vinyl alcohol) thin films, where the aggregation does not develop beyond the formation of dimers even at very high dye concentrations.[16,30]

Figure 4 presents numerically deconvoluted absorption spectrum of Rh6G dimers in TiO_2 film together with the

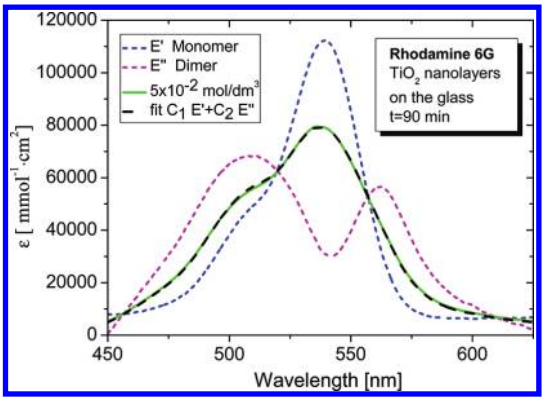

Figure 4. Numerically deconvoluted absorption spectra of Rh6G/TiO_2 dimers and monomers, the measured total absorption spectrum at $c = 5 \times 10^{-2}$ mol/dm^3, and the numerical fit.

monomer spectrum and an example of the fitted spectrum to the measured absorption spectrum at $c = 5 \times 10^{-2}$ mol/dm^3. Calculations were based on our software using the procedures described previously.[16,17,30] It can be seen from the figure that the Rh6G dimer absorption spectrum consists of two bands: the H band with the maximum at 509 nm and the J band with the maximum at 563 nm. In the case studied the H and J bands are not fully spectrally separated, which resembles also the case of Rh6G in water,[9] but not in poly(vinyl alcohol) films[17] or ethylene glycol.[16]

The obtained value of Davydov exciton splitting $\Delta\nu$ = 1884 cm^{-1} for H and J bands for Rh6G/TiO_2 is, in turn, close to that in poly(vinyl alcohol) film,[17] $\Delta\nu$ = 1881 cm^{-1}, or ethylene glycol,[16] $\Delta\nu$ = 1800 cm^{-1}, but it is somewhat larger than in Langmuir–Blodgett films,[31] $\Delta\nu$ = 1750 cm^{-1}, and distinctly larger than in water,[9] $\Delta\nu$ = 1500 cm^{-1}, and glycerol,[32] $\Delta\nu$ = 1079 cm^{-1}. The value of $\Delta\nu$ = 1884 cm^{-1} obtained in this work exceeds also significantly the halfwidth $\Delta\nu'$ = 1400 cm^{-1} of the monomer absorption band of Rh6G/TiO_2 suggesting strong coupling of the system investigated for which vibronic interactions are negligible. Based on the locations of spectral peaks and the value of splitting, one can calculate the angle α between the transition moments of the monomer units in the dimer as well as the separation distance between the monomers in the dimer for Rh6G/TiO_2. Since in the case of interest the H band is stronger than the J band we can apply the parallel plane model for the dimer.[33,34] The value of α can be determined from the relation:[34]

$$\alpha = 2\tan(f^{J}\nu^{H}/f^{H}\nu^{J})^{1/2} \quad (1)$$

where f^J and f^H denote the oscillator strengths of the J and H bands, respectively. In the case of Rh6G/TiO_2 we obtained the value of α = 600. This value can be compared to those obtained for ethylene glycol and poly(vinyl alcohol) films, where Rh6G dimers were found to be fluorescent. In the case studied it is somewhat higher than that of Rh6G in ethylene glycol (α = 490), but smaller than for Rh6G in poly(vinyl alcohol) films (α = 740).[16,17] Also the monomer separation distance R can be easily obtained from the relation valid for the parallel plane model:

$$R = (2.14 \times 10^{10} f^{M} \cos\alpha/\nu \times \Delta\nu)^{1/3} \quad (2)$$

dx.doi.org/10.1021/jp3022562 | J. Phys. Chem. C 2012, 116, 12304–12311

where f^M denotes the oscillator strength of the monomer. For Rh6G/TiO_2 we obtained the value R = 6.1 Å which is close to the value for Rh6G in other media, for example, in ethylene glycol (6.8 Å). Furthermore, it should be stressed that assuming proper gelation time of the solution is very important because it introduces a significant change in practically all spectral characteristics, especially at higher concentrations of the dye. The spectroscopic results, repeated many times by us, show that there exists certain gelation time after which further change in the fluorescence and absorption spectra becomes insignificant. However, one has to be aware that the gelation process can slowly continue even at very long time scales.

Figures 5 and 6 show the absorption spectra of Rh6G/TiO_2 (Figure 5) and Rh6G/SiO_2 (Figure 6) at the highest

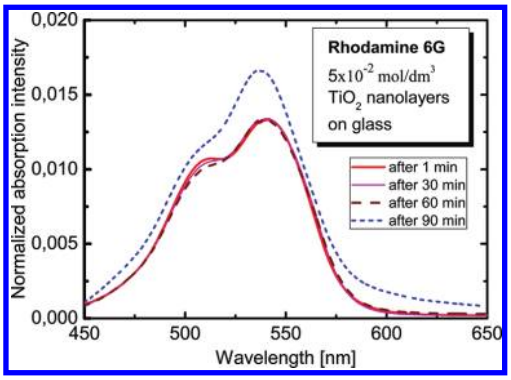

Figure 5. Effect of the gelation time on the absorption spectra of Rh6G/TiO_2 at the highest concentration $c = 5 \times 10^{-2}$ mol/dm^3.

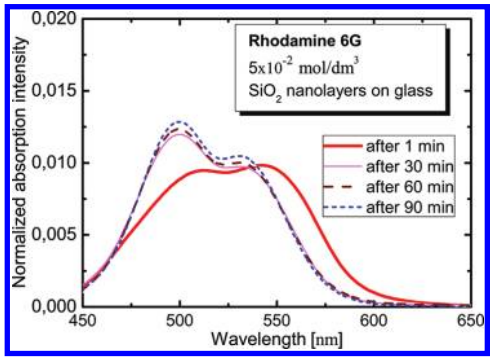

Figure 6. Effect of the gelation time on the absorption spectra of Rh6G/SiO_2 at the highest concentration $c = 5 \times 10^{-2}$ mol/dm^3.

concentration $c = 5 \times 10^{-2}$ mol/dm^3 for a couple of different gelation times. It can be seen from both figures that for the gelation time t = 90 min the highest maximal absorbance values are obtained. At longer times no further significant changes in absorption profile and its intensity were found; therefore we assumed the gelation time t = 90 min as a reference one and present all further spectroscopic results for this particular gelation time. More detailed studies on this subject performed by us indicate that for silica matrices absorption spectra exhibit almost constant intensity and shape for the gelation time even as short as 30 min. However, for TiO_2 matrices a significant change in absorption intensity is observed only between 60 and 90 min. In this latter case the change in absorption spectrum profile is much more subtle than for SiO_2 matrix. This latter observation can be attributed to the precursor substituent effect. Figures 7 and 8 shows the difference between both substituents in TiO_2 (Figure 7) and SiO_2 (Figure 8) matrices.

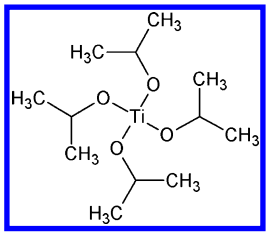

Figure 7. Structural formula of TiO_2 precursor, titanium(IV) tetra(2-propanolate).

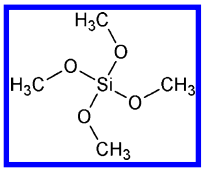

Figure 8. Structural formula of SiO_2 precursor, tetramethyl orthosilicate.

The Si precursor possesses methyl groups, whereas the Ti precursor possesses propyl groups, which are branched and more complex. This leads to the steric effect resulting in the lowered velocity of precursor hydrolysis and a longer gelation time.

Figures 9 and 10 shows selected fluorescence spectra of the Rh6G/TiO_2 (Figure 9) and Rh6G/SiO_2 (Figure 10) matrix at

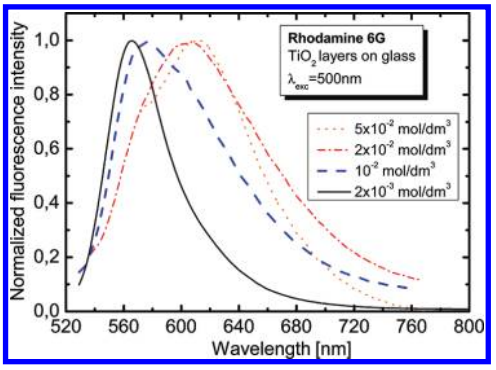

Figure 9. Fluorescence spectra of Rh6G/TiO_2 nanolayers at several selected concentrations for the dye at room temperature, T = 293 K.The excitation wavelength was 500 nm.

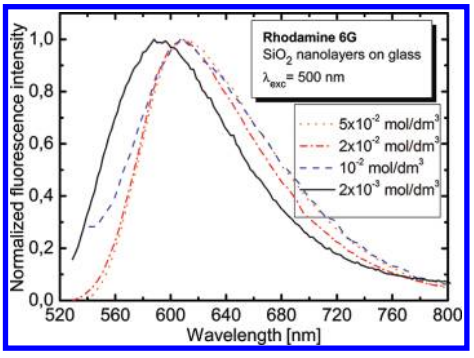

Figure 10. Fluorescence spectra of Rh6G/SiO_2 nanolayers at several selected concentrations for the dye at room temperature, T = 293 K.The excitation wavelength was 500 nm.

several dye concentrations. As seen from Figure 9 for Rh6G/TiO_2 nanolayers the observed changes in the fluorescence spectra at high dye concentrations are distinct. The maximum

dx.doi.org/10.1021/jp3022562 | J. Phys. Chem. C 2012, 116, 12304−12311

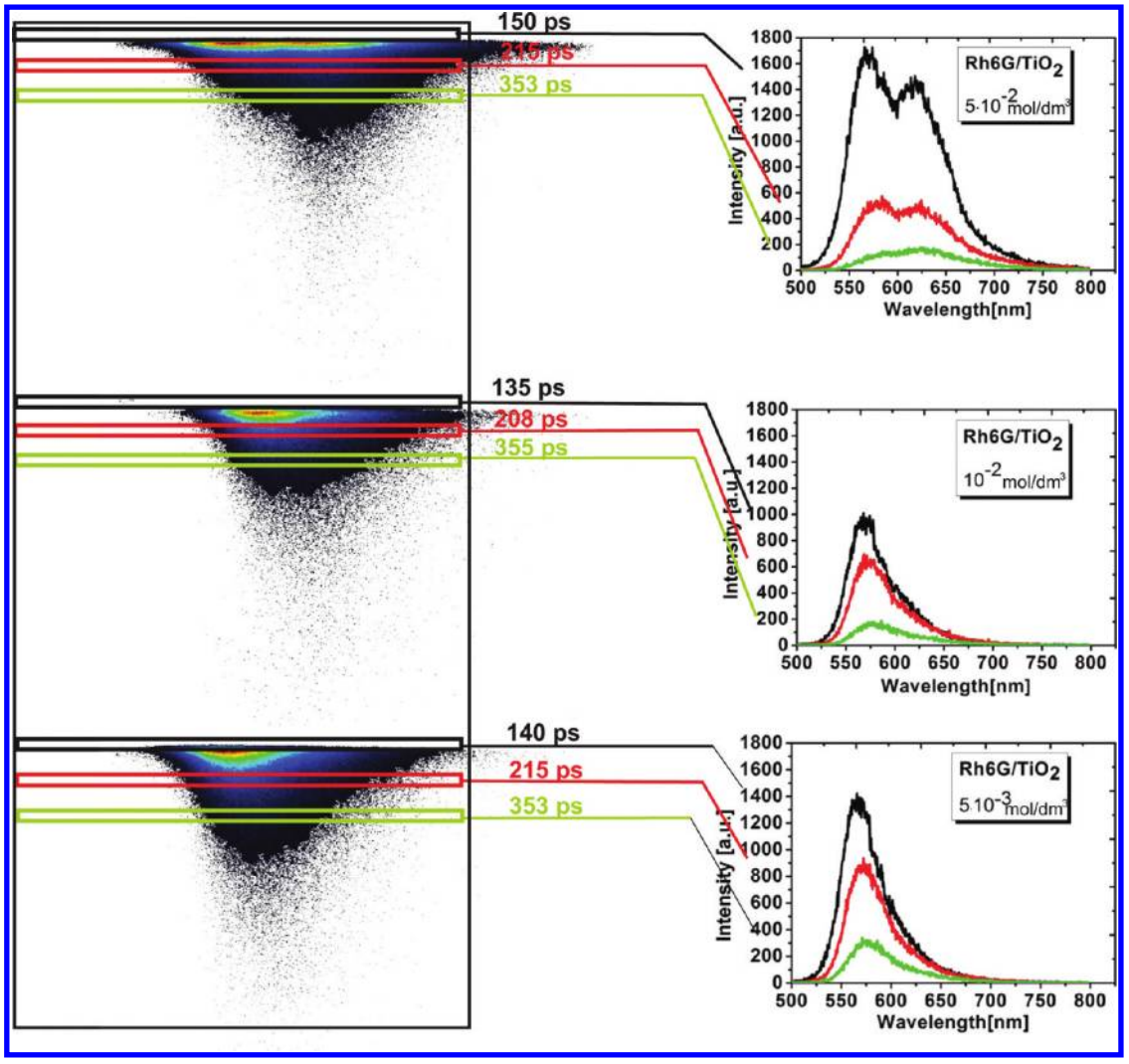

Figure 11. Time-resolved emission spectra of Rh6G/TiO_2 nanolayers at several selected concentrations of the dye at room temperature T = 293 K. The excitation wavelength was 485 nm.

of fluorescence spectrum for Rh6G/TiO_2 shifts from 566 nm at $c = 2 \times 10^{-3}$ mol/dm^3 to 612 nm for $c = 5 \times 10^{-2}$ mol/dm^3. Such a strong red shift of Rh6G/TiO_2 fluorescence spectrum is accompanied by the formation of a new fluorescence band at the long wave side of the spectrum with the maximum at 612 nm. This profile change is very similar to that observed for Rh6G in ethylene glycol, thin poly(vinyl alcohol) films and porous silica materials at high dye concentrations, where it has been attributed to fluorescent J aggregates.[16,17,20] From Figure 10 the red shift of Rh6G/SiO_2 fluorescence spectrum can also be seen with the increase in concentration. This time the fluorescence maximum shifts from about 591 nm ($c = 2 \times 10^{-3}$ mol/dm^3) to 611 nm ($c = 5 \times 10^{-2}$ mol/dm^3). The location of this latter peak is very similar to that of Rh6G/TiO_2. This 20 nm shift in the case of Rh6G/SiO_2 is accompanied by a much smaller change of emission profile. Because of low optical density of the samples (below 0.1), the observed spectral shifts in Figures 9 and 10 cannot be attributed to inner filter effects.

However, in a porous rigid medium one could expect that inhomogeneous orientational broadening of energy levels takes place and contributes to the red shift observed. Such an effect has been found previously for several fluorophores in thin poly(vinyl alcohol) films and viscous solutions.[16,35−37] The molecular neighborhood of fluorophores in complex media can differ significantly from one molecule to another resulting in a stronger or weaker solute−solvent interaction. If inhomogeneous broadening takes place, fluorescence spectra shift to the red with the increasing excitation wavelength. Therefore, we checked, if the emission spectra of Rh6G/TiO_2 and Rh6G/SiO_2 at low concentrations are sensitive to the excitation wavelength. However, only a slight shift of fluorescence spectra maximum was found for the systems herein studied at room temperature, which is a clear though somewhat surprising indication that inhomogeneous orientational broadening should not contribute significantly to the fluorescence shifts upon experimental conditions. Also the results of emission anisotropy measurements performed both in excitation and emission bands do not indicate any significant effects of inhomogeneous broadening. The obtained emission anisotropy spectra were flat and did not increase with excitation wavelength, which would have been an indication of inhomogeneous broadening effect. The emission anisotropies at the highest dye concentration were also rather low (r about 0.05) due to strong multistep energy migration. From the results presented one can conclude that the aggregates formed in the ground state contribute significantly to the fluorescence of Rh6G/TiO_2 and could contribute to

dx.doi.org/10.1021/jp3022562 | J. Phys. Chem. C 2012, 116, 12304−12311

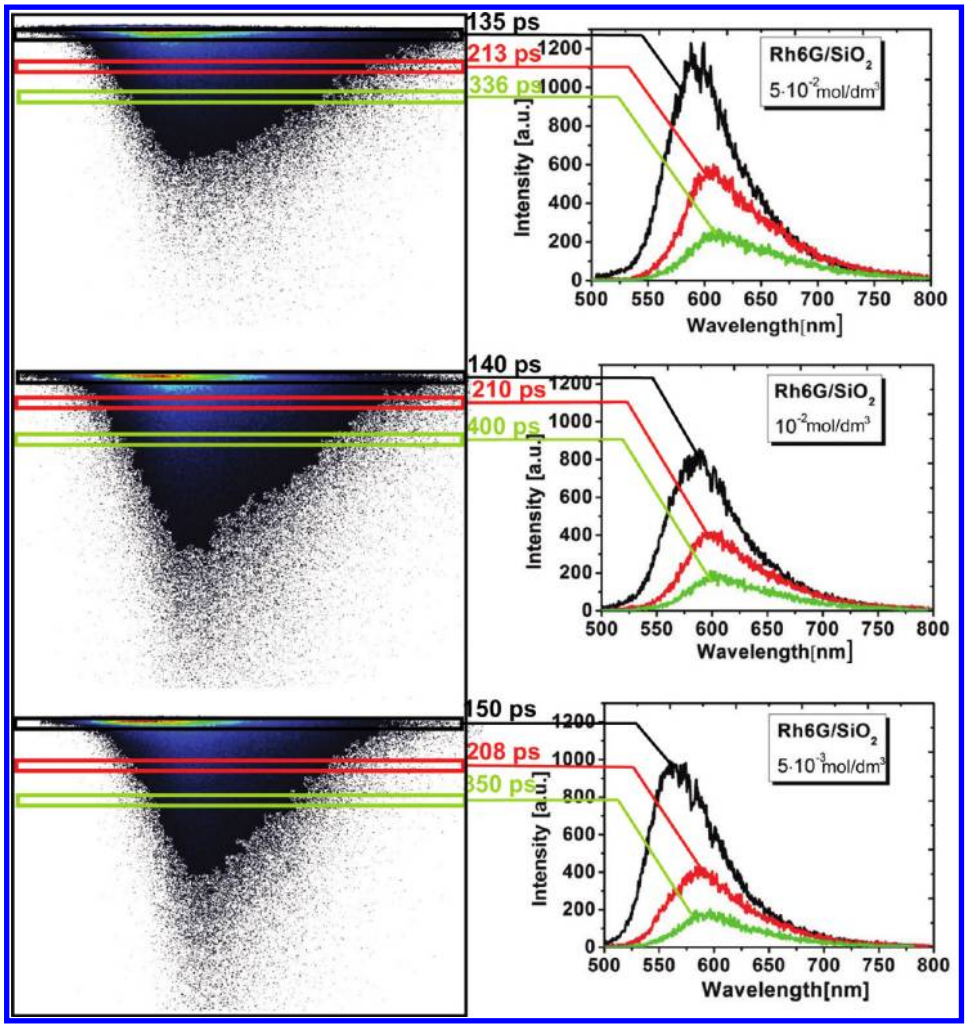

Figure 12. Time-resolved emission spectra of Rh6G/SiO_2 nanolayers at several selected concentrations of the dye at room temperature T = 293 K. The excitation wavelength was 485 nm.

some extent to the fluorescence of Rh6G/SiO_2. By comparison with the results reported in the other mentioned works we can also conclude that the observed changes in fluorescence spectra profiles in the nanolayers are weaker compared to those in bulk materials. Also our preliminary results of fluorescence characteristics performed for Rh6G/TiO_2 bulk materials at high dye concentrations suggest that in such bulk materials the reabsorption can to some extent contribute to the emission profile change (to be reported separately). Until now a majority of the works devoted to the aggregate formation in porous materials have been made using only the steady-state spectroscopic techniques. Therefore, it is interesting to present some results of the time evolution of Rh6G/TiO_2 and Rh6G/SiO_2 emission spectra measured with our state of the art pulsed spectrofluorometer. Selected results for Rh6G/TiO_2 and Rh6G/SiO_2 matrix are given in Figures 11 and 12, respectively.

On the left of both subfigures original images taken from the streak camera at three representative dye concentrations are presented. At these images vertical direction corresponds to time, horizontal direction to wavelength, and colors reflect emission intensity. All measurements were made in a 5 ns time window. The red color correspond to the highest intensities, whereas the black color corresponds to the lowest fluorescence intensity. Slicing the image horizontally yields fluorescence spectrum at a given time moment after the excitation (cp. the figure). The upper panels in the figures correspond to the highest concentration $c = 5 \times 10^{-2}$ mol/dm^3, the middle ones to $c = 10^{-2}$ mol/dm^3, and the lowest panels correspond to the concentration $c = 5 \times 10^{-3}$ mol/dm^3. From Figure 11 (corresponding to Rh6G/TiO_2 nanolayers) one can see that at the highest concentration the emission spectrum (upper panel) consists of two bands even at quite short times after excitation. It is visible that the spectrum evolves with time from the relative monomer and dimer peak intensities. At shorter time (150 ps) monomer fluorescence with a peak at 569 nm is dominant over the dimer fluorescence with a peak at 618 nm; at intermediate times (215 ps) the fluorescence intensities of monomers and dimers are similar, while for the longest time (353 ps) the dimer fluorescence is somewhat stronger. This regularity results from monomer to dimer energy transfer developing with time. The observed peak locations of monomers and dimers are similar to those from the steady-state fluorescence spectra. It should be noted that we found slight time dependence of the monomer and dimer peak locations. The dimer fluorescence peak shifts about 10 nm to the red at long times (to 628 nm) and the monomer peak about 17 nm (to 586 nm). This latter shift may result from the spectral overlap between monomers and dimers and to some extent from the dynamic effect of inhomogeneous broadening of energy levels.[36,37] This latter slight effect seems to be

confirmed by a 9 and 6 nm shifts of monomer fluorescence peaks with time also at $c = 10^{-2}$ mol/dm^3 and $c = 5 \times 10^{-3}$ mol/dm^3, respectively. In the case of Rh6G/SiO_2 nanolayers (Figure 12) one can mostly see the strong shift of a single peak fluorescence band with time. At the lowest concentration $c = 5 \times 10^{-3}$ mol/dm^3 this shift is very pronounced (from 560 nm at $t = 150$ ps to 593 at $t = 350$ ps), but it is much smaller at higher Rh6G concentrations [(from 588 nm (140 ps) to 602 nm (400 ps)] for $c = 10^{-2}$ mol/dm^3 and from 593 nm (135 ps) to 610 nm (330 ps) for $c = 5 \times 10^{-2}$ mol/dm^3. This result indicates a stronger dynamical effect of inhomogeneous broadening of energy levels occurring at quite short time scale and therefore weakly visible in steady-state fluorescence spectra experiments.

To visualize the described changes in the fluorescence spectrum profile with time, Figures 13 and 14 show the

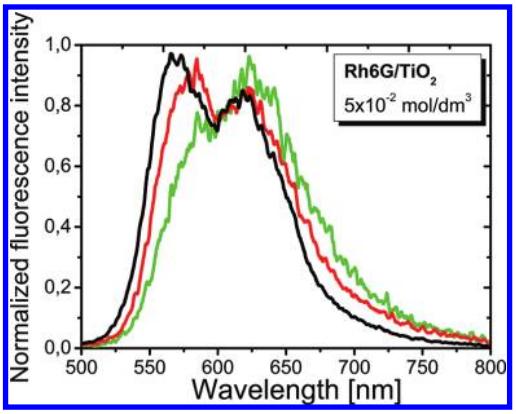

Figure 13. Normalized time-resolved emission spectra of Rh6G/TiO_2 nanolayers at the highest dye concentration. The excitation wavelength was 485 nm.

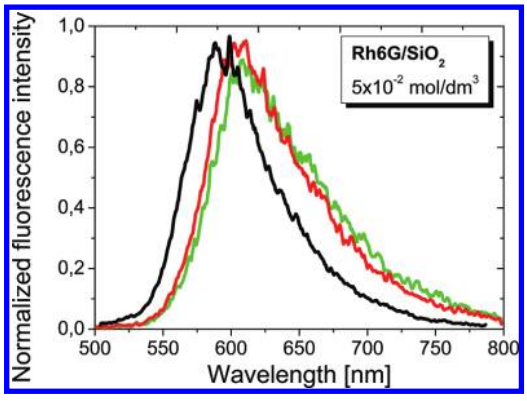

Figure 14. Normalized time-resolved emission spectra of Rh6G/SiO_2 nanolayers at the highest dye concentration. The excitation wavelength was 485 nm.

normalized time-resolved fluorescence spectra of Rh6G/TiO_2 and Rh6G/SiO_2 for the most concentrated samples, respectively. Indeed, it can be seen from the figure that the time evolution of emission spectra for Rh6G/TiO_2 and Rh6G/SiO_2 is of a different character. In the case of Rh6G/TiO_2 (Figure 13) the shift of the emission maximum to the red is accompanied by a strong change in the emission profile, whereas in the case of Rh6G/SiO_2 (Figure 14) this is mostly the emission maximum shift with only a slight change in the emission profile. The mean fluorescence lifetime of R6G in the absence of aggregates is 4 ns.[30] For R6G/TiO_2 it shortens at high concentration $c = 5 \times 10^{-2}$ mol/dm^3 to 60 ps (at 570 nm) and to 73 ps at 618 nm corresponding approximately to the emission maximum of the dimer. For R6G/SiO_2 it is about 46 ps at 570 nm and about 96 ps at 618 nm. This observation wavelength dependence of the mean fluorescence lifetime suggests a certain contribution of aggregates to the emission signal also in the case of R6G/SiO_2. However, it should be noted that at the present stage it is difficult to attribute this mean lifetime or its components to pure aggregate fluorescence, because we deal with a complex system of fluorescent monomers and aggregates coupled through energy transport processes.

CONCLUSION

Based on the sol−gel method it was possible to obtain high-quality hybrid luminescent nanolayers. The formation of fluorescent Rh6G aggregates at high dye concentrations was found based on various steady-state and time-resolved spectroscopic techniques. The reabsorption-free nanolayers enable much more reliable evaluation of the nature of concentration-dependent phenomena and aggregate photophysical properties compared to bulk materials, where inner filter effects are usually strong. In the case of Rh6G/TiO_2, which is of primary interest to us, it can be concluded that Rh6G dimers are formed based on the concentration dependence of absorption spectra. The basic structural information on these dimers was provided and compared to other media. The dimers are fluorescent with the emission maximum shifted significantly to the red which suggests that the dimers fluorescence originates from the lower J level. In the case of Rh6G/SiO_2, however, the changes observed in the absorption spectra are more pronounced and different in character. The absence of the isosbestic points suggests the formation of more complex aggregates. This is also reflected in a different character of fluorescence spectra changes with concentration than in the case of Rh6G/TiO_2. This time, the changes in the fluorescence spectra are more subtle and mostly concern the spectral shift to the red with only a slight change in the emission profile. The observed regularities for both types of nanolayers in steady-state experiments are fully consistent with those of time-resolved emission spectra.

To define the hybrid material and to compare the results obtained in different laboratories well, it is extremely important to perform all presented experiments for a given gelation time. It was shown that aggregation in hybrid materials strongly depend on gelation time. However, there exists a certain gelation time which can be considered a reasonable limiting time above which further changes in absorption and fluorescence characteristics become insignificant (around 90 min in the case studied). Such important information is usually omitted in scientific papers, which can be one of the main reasons that the results obtained for hybrid nanomaterials differ between laboratories.

AUTHOR INFORMATION

Corresponding Author

*E-mail: fizpb@ug.edu.pl. Phone: +48 (0)58 5232221. Fax: +48 (0)58 3413175.

Notes

The authors declare no competing financial interest.

■ ACKNOWLEDGMENTS

This research has been partly supported within the International Ph.D. Project "Physics of Future Quantum-Based Information Technologies" (MPD/2009-3/4) financed by Foundation for Polish Science (A.L.) and from European Social Fund as a part of the project "Educators for the Elite—Integrated Training Program for PhD Students, Postdocs and Professors As Academic Teachers at University of Gdansk" within the framework of Human Capital Operational Programme, Action 4.1.1, Improving the Quality of Educational Offer of Tertiary Education Institutions (A.S.). The authors thank K. Lenczewska for help during some measurements and preparation of the samples.

■ REFERENCES

(1) Grobelna, B.; Bojarski, P. *J. Non-Cryst. Solids* **2009**, *355*, 2309−2313.
(2) Reisfeld, R. *J. Lumin.* **1997**, *7*, 72−74.
(3) Reisfeld, R. *Opt. Mater.* **2010**, *32*, 850−856.
(4) Jiang, L.; Feng, L. *Bioinspired intelligent nanostructured interfacial materials*; World Scientific Publishing Company: Beijing, China, 2010.
(5) Gratzel, M. *Nature* **1991**, *353*, 737−740.
(6) Lili, H.; Zhonghong, J. *Opt. Commun.* **1998**, *148*, 275−280.
(7) Reisfeld, R. *Opt. Mater.* **2001**, *16*, 1−7.
(8) Palomino-Merino, R.; Torres-Kauffman, J.; Lozada-Morales, R.; Portillo-Moreno, O.; Garcia-Rocha, M.; Zelaya-Angel, O. *Vacuum* **2007**, *81*, 1480−1483.
(9) Bojarski, C.; Obemueller, G. *Acta Phys. Pol., A* **1976**, *50*, 389−411.
(10) Obemueller, G.; Bojarski, C. *Acta Phys. Pol., A* **1977**, *52*, 431.
(11) Arbeloa, F. L.; Gonzalez, I. L.; Ojeda, P. R.; Arbeloa, I. L. *J. Chem. Soc., Faraday Trans. II* **1982**, *78*, 989−994.
(12) Ojeda, P. R.; Amashta, I. A. K.; Ochoa, J. R.; Arbeloa, I. L. *J. Chem. Soc., Faraday Trans. II* **1988**, *84*, 1−8.
(13) Taguchi, T.; Hirayama, S.; Okamoto, M. *Chem. Phys. Lett.* **1994**, *231*, 561−568.
(14) Vogel, R.; Meredith, P.; Harvey, M. D.; Rubinsztein-Dunlop, H. *Spectrochim. Acta, Part A* **2004**, *60*, 245−249.
(15) Vogel, R.; Meredith, P.; Kartini, I.; Harvey, M.; Riches, J. D.; Bishop, A.; Heckenberg, N.; Trau, M.; Rubinsztein-Dunlop, H. *ChemPhysChem* **2003**, *4*, 595−603.
(16) Bojarski, P.; Matczuk, A.; Bojarski, C.; Kawski, A.; Kukliński, B.; Żurkowska, G.; Diehl, H. *Chem. Phys.* **1996**, *210*, 485−499.
(17) Bojarski, P. *Chem. Phys. Lett.* **1997**, *278*, 225−232.
(18) Vodolazskaya, I. V.; Krasheninnikov, V. V.; Saletsky, A. M. *Appl. J. Spectrosc.* **2011**, *78*, 149−154.
(19) Salleres, S.; Arbeloa, F. L.; Martinez, V. M.; Arbeloa, T.; Arbeloa, I. L. *Langmuir* **2010**, *26*, 930−937.
(20) Carbonaro, C. M.; Meinardi, F.; Ricci, P. C.; Salis, M.; Anedda, A. *J. Phys. Chem. B* **2009**, *113*, 5111−5116.
(21) Malfatti, L.; Kidchob, T.; Aiello, D.; Aiello, R.; Testa, F.; Innocenzi, P. *J. Phys. Chem. C* **2008**, *112*, 16225−16230.
(22) del Monte, F.; Mackenzie, J. D.; Levy, D. *Langmuir* **2000**, *16*, 7377−7382.
(23) Carbonaro, C. M. *J. Photochem. Photobiol., A* **2011**, *222*, 56−63.
(24) Ketskemety, I.; Dombi, J.; Horvai, R.; Hevesi, J.; Kozma, L. *Acta Phys. Chem. (Szeged)* **1961**, *7*, 17−21.
(25) Rangełowa-Jankowska, S.; Jankowski, D.; Grobelna, B.; Gryczyński, I.; Gryczyński, Z.; Bogdanowicz, R.; Bojarski, P. *ChemPhysChem* **2011**, *12*, 2449−2452.
(26) Kawski, A.; Piszczek, G.; Kukliński, B.; Nowosielski, T. *Z. Naturforsch.* **1994**, *49a*, 824−828.
(27) Kubicki, A. *Exp. Tech. Phys.* **1989**, *37*, 329−333.
(28) Bojarski, P.; Kawski, A. *J. Fluoresc.* **1992**, *2*, 133−139.
(29) Kubicki, A. A.; Bojarski, P.; Grinberg, M.; Sadownik, M.; Kukliński, B. *Opt. Commun.* **2006**, *263*, 275−280.
(30) Bojarski, P.; Matczuk, A.; Kułak, L.; Bojarski, C. *Asian J. Spectros.* **1999**, *5*, 1−21.
(31) Vuorimaa, E.; Ikonen, M.; Lemmetyinen, H. *Chem. Phys.* **1994**, *188*, 289−302.
(32) Levshin, V. L.; Baranova, E. G. *Opt. Spectrosc.* **1959**, *6*, 31−36.
(33) McRae, E. G.; Kasha, M. *J. Chem. Phys.* **1958**, *28*, 721−722.
(34) Kasha, M.; Rawls, H. R.; El Bayoumi, A. *Pure Appl. Chem.* **1965**, *11*, 371−392.
(35) Nemkovich, N.; Rubinov, A. N.; Tomin, V. I.; Lakowicz, J. R., Eds. In *Topics in Fluorescence Spectroscopy*; Plenum Press, New York, 1991; p 367.
(36) Grajek, H. *Curr. Top. Biophys.* **2011**, *12*, 1−13.
(37) Bojarski, P.; Kułak, L.; Bojarski, C.; Kawski, A. *J. Fluoresc.* **1995**, *5*, 293−297.